Coupled phase transformation, chemical decomposition, and deformation in plastic-bonded explosive: Models

Valery I. Levitas[a)]
Department of Mechanical Engineering, Texas Tech University, Lubbock, Texas 79409, USA

Bryan F. Henson, Laura B. Smilowitz, David K. Zerkle, and Blaine W. Asay
Los Alamos National Laboratory, Los Alamos, New Mexico 87545, USA

(Received 30 June 2007; accepted 1 October 2007; published online 4 December 2007)

A continuum thermomechanochemical model of the behavior of a plastic-bonded explosive (PBX) 9501 formulation consisting of the energetic crystal octahydro-1,3,5,7-tetranitro-1,3,5,7-tetrazocine (HMX) embedded in a polymeric binder is developed. Our main focus is on the study of the $\beta \leftrightarrow \delta$ phase transformations (PTs) in crystalline HMX under a complex pressure-temperature path. To reproduce the pressure-temperature path, in particular during heating of PBX inside of a rigid cylinder, the $\beta \leftrightarrow \delta$ PTs in HMX are coupled to chemical decomposition of the HMX and binder leading to gas formation, gas leaking from the cylinder, elastic, thermal, and transformational straining as well as straining due to mass loss. A fully physically based thermodynamic and kinetic model of the $\beta \leftrightarrow \delta$ PT in HMX crystal is developed. It is based on a suggested nucleation mechanism via melt mediated nanocluster transformation and the recently revealed growth mechanism via internal stress-induced virtual melting. During the nucleation, nanosize clusters of the β phase dissolve in a molten binder and transform diffusionally into δ phase clusters. During the interface propagation, internal stresses induced by transformation strain cause the melting of the stressed δ phase much below (120 K) the melting temperature and its immediate resolidification into the unstressed δ phase. These mechanisms explain numerous puzzles of HMX polymorphism and result in overall transformation kinetics that is in good agreement with experiments. Simple phenomenological equations for kinetics of chemical decomposition of the HMX and the binder are in good correspondence with experiments as well. A continuum deformation model is developed in two steps. The geometrically linear (small strain) theory is used to prove that the internal stresses and macroscopic shear stresses are negligible. Then a large strain theory is developed under hydrostatic loading. The developed continuum thermomechanochemical model is applied in the accompanying paper [V. I. Levitas, B. F. Henson, L. B. Smilowitz, D. K. Zerkle, and B. W. Asay, J. Appl. Phys. (submitted)] to modeling the heating of PBX inside of a rigid cylinder. © *2007 American Institute of Physics*.
[DOI: 10.1063/1.2817616]

I. INTRODUCTION

PBX 9501 is an important high explosive with wide applications that is currently under intensive study in governmental laboratories and academia. The PBX 9501 formulation consists of 94.9% by weight of the organic energetic crystals octahydro-1,3,5,7-tetranitro-1,3,5,7-tetrazocine (HMX) with the remainder being a polymeric binder. The binder consists of 2.5% of Estane, 2.5% nitroplasticizer, and 0.1% antioxidant. Prediction of the thermomechanochemical behavior of PBX under various temperature-pressure loading histories in a preignition regime is of great importance for the safety of its storage, transportation, and handling. This is difficult without the understanding and the ability to model actual chemical, physical, and mechanical processes that occur in the HMX and binder during thermomechanical loading. We will focus on the study of the reconstructive $\beta \leftrightarrow \delta$ in crystalline HMX under complex pressure-temperature paths. The $\beta \rightarrow \delta$ PT starts above 432 K at ambient pressure. This PT is accompanied by 8% of transformation volume expansion which produces huge internal stresses within HMX that affect the transformation thermodynamics, kinetics and microstructure. Such a volume change also creates internal stresses within the PBX formulation as well as within a macroscopic sample if its deformation is restricted (for example, by rigid walls). Knowledge of the kinetics of the $\beta \leftrightarrow \delta$ phase transformation (PT) equation is very important not only because of these stresses but also because of the greater sensitivity[1] and different properties of the δ phase.

There are a number of phenomenological kinetic models for the $\beta \leftrightarrow \delta$ PT.[2–5] The main drawback of any phenomenological model is the impossibility to apply it beyond the region of parameters (temperature and pressure evolution) where it is directly confirmed experimentally. In most cases, these data are generated in isothermal experiments under zero pressure.[2–5] In two particular cases of experiments under high pressure,[6,7] the results are not well understood. In one experiment at high temperatures,[6] the slope of the thermodynamically calculated $\beta - \delta$ equilibrium line contradicts

[a)]Author to whom correspondence should be addressed. Electronic mail: valery.levitas@ttu.edu.

known experimental data. In another,[7] the beta-delta phase transition is observed at temperatures well below the equilibrium temperature subsequent to the release of a pressurized sample. In contrast, the extension of physical mechanism-based models beyond the range of parameters where they are checked experimentally is much more reliable.

Along this direction, we revealed recently[8–10] that the $\beta \leftrightarrow \delta$ PT in the HMX energetic crystal occurs via the virtual melting mechanism. The virtual melting mechanism has been incorporated into several kinetic models by combination with several phenomenological nucleation models.[8,10,11] As will be shown in Sec. IV in Ref. 12, even the most advanced kinetic model using a phenomenological nucleation kinetics[10,11] exhibits contradictory results when applied to either the high pressure regime or cyclic PT. In the current paper we further developed a suggested physical nucleation mechanism in HMX via melt mediated nanocluster transformation.[13] It allows us to explain extremely unusual nucleation occurring very close (0.6 K) to the phase equilibrium temperature θ_e. A combination of nucleation kinetics based on this mechanism and the growth kinetics based on virtual melting results in a fully physical model for the overall transformation kinetics.

To reproduce complex pressure-temperature paths, in particular during heating of PBX inside of a rigid cylinder, the $\beta \leftrightarrow \delta$ PTs in HMX are coupled to other chemical and mechanical processes. They include: chemical decomposition of the HMX, nitroplasticizer, and Estane leading to gas production, gas leaking from the closed volume, and deformations of PBX constituents in solid, liquid, and gas form. When these processes (including the $\beta \leftrightarrow \delta$ PTs) occur in a closed volume, they are coupled through the pressure generated by thermal expansion, transformation strain, mass loss due to chemical decomposition, and gas leaking, as well as gas formation in a closed volume. Development of such a coupled thermomechanochemical model and its application in numerical simulations of the earlier mentioned processes is the main goal of the current two-part paper.

The paper is organized in the following way. In Sec. II, the main thermodynamic functions for the $\beta \rightarrow \delta$ PT and melting of the β and δ phases are presented. They are used in subsequent sections to develop a physically based nucleation and growth kinetics for the $\beta \rightarrow \delta$ PT. In Sec. III, a nucleation mechanism for reconstructive solid-solid PT in HMX via melt mediated nanocluster transformation is described. The kinetic equation for nucleation is derived under variable temperature and pressure. We initially reported on this mechanism in a short letter.[13]

In Sec. IV, the kinetic equations for the $\beta-\delta$ interface velocity and volume fraction of the δ phase due to growth are derived based on the virtual melting growth mechanism.[8–10] In Sec. V, both nucleation and growth kinetics are combined to model the overall kinetics of the $\beta \rightarrow \delta$ PT. The temperature dependence of both interface propagation velocity and volume fraction of the δ phase is in good agreement with various experiments under isothermal conditions and zero pressure. In Sec. V, a continuum mechanical model for a composite consisting of an HMX crystal embedded in a binder with allowance for the $\beta \rightarrow \delta$ PT and chemical decomposition of the HMX and binder is developed. This problem is approached in two steps. First, we show based on geometrically linear (i.e., small strain) theory that the effect of the shear modulus of the binder and internal stresses between the HMX and the binder can be neglected, i.e., the composite can be considered as a hydrostatic medium. This simplification allowed us to develop an exact, geometrically nonlinear theory that correctly takes into account all finite and large strains. In Sec. VII, simple phenomenological models for chemical decomposition of the HMX and binder and for gas leaking are formulated. Equations for the kinetics of chemical decomposition of the nitroplasticizer and Estane are in good correspondence with temperature ramp experiments at constant heating rate. Kinetic equations for all chemical decomposition processes in PBX describe the isothermal experimental data well. An equation of state for the resulting gas phase is formulated. An expression for pressure in PBX is derived that takes into account the coupling of all thermomechanochemical processes. Section VIII contains the concluding remarks. In the accompanying paper,[12] the results of the simulation of coupled phase transformation, chemical decomposition and deformation in PBX 9501 during heating inside of a rigid cylinder are presented.

II. THERMODYNAMICS OF $\beta-\delta$ PHASE TRANSFORMATION AND MELTING IN HMX

Along the lines described in Refs. 8, 10, and 11, we determine the thermodynamic functions necessary for the development of our kinetic models. The molar thermodynamic driving force for the $\beta \rightarrow \delta$ PT is

$$-\Delta g_{\beta\rightarrow\delta} = -(\Delta h_{\beta\rightarrow\delta} - \theta \Delta s_{\beta\rightarrow\delta}) - p\Delta v_{\beta-\delta}, \tag{1}$$

where $\Delta g_{\beta\rightarrow\delta}$, $\Delta h_{\beta\rightarrow\delta}$, $\Delta s_{\beta\rightarrow\delta}$, and $\Delta v_{\beta-\delta}$ are the change in the molar Gibbs potential, enthalpy, entropy, and volume during the $\beta \rightarrow \delta$ PT, θ is the temperature, and p is the pressure. Since the maximum pressure at which the $\beta \rightarrow \delta$ PT is possible is less than 0.245 GPa (pressure at the triple point, see Ref. 11) and the bulk modulus is $B=15$ GPa,[14] the pressure dependence of the bulk moduli in such a pressure range can be neglected. The change in elastic energy is then defined as $0.5p^2(1/B_\beta - 1/B_\delta)$. Since literature values of the bulk moduli of HMX differ significantly,[14,15] and since the difference between B_δ and B_β should be relatively small, the change in elastic energy is neglected in Eq. (1).

We note that there is some scatter in the thermodynamic data, however, assuming constant transformation enthalpy $\Delta h_{\beta\rightarrow\delta}=9.8$ kJ/mol,[2,3] and the entropy related to enthalpy through phase equilibrium temperature $\theta_e=432$ K (within a range given in Refs. 16 and 17), i.e., $\Delta s_{\beta\rightarrow\delta}=\Delta h_{\beta\rightarrow\delta}/\theta_e = 22.68$ J/mol K, we obtain

$$-\Delta g_{\beta\rightarrow\delta} = \Delta s_{\beta\rightarrow\delta}(\theta - \theta_e) - p\Delta v_{\beta-\delta}. \tag{2}$$

Note that the phase equilibrium temperature may depend on impurities (in particular, RDX). We choose $\theta_e=432$ K since it provides the best fit for the various interface velocity experiments (see Refs. 9–11). Since volumetric transformation strain $\varepsilon^t=\rho_\beta/\rho_\delta-1$, then

$$\Delta v_{\beta-\delta} = M\left(\frac{1}{\rho_\delta} - \frac{1}{\rho_\beta}\right) = \frac{M}{\rho_\beta}\left(\frac{\rho_\beta}{\rho_\delta} - 1\right) = M\frac{\varepsilon^t}{\rho_\beta}, \tag{3}$$

where $M \simeq 0.296$ kg/mol is the HMX molecular weight and $\varepsilon^t = 0.08$;[14] the mass density of the β phase at phase equilibrium temperature $\theta = 432$ K is estimated by equation $\rho_\beta = 1905/(1+\varepsilon_\beta^\theta) = 1873$ kg/m^3, where the mass density at 300 K is 1905 kg/m^3 (Ref. 18) and ε_β^θ is determined in Ref. 19 [see Eq. (47)]; the mass density of the δ phase at $\theta = 432$ K is $\rho_\beta = \rho_\beta/(1+\varepsilon_0^t) = 1734$ kg/m^3. Then $\Delta v_{\beta-\delta} = 1.264 \times 10^{-5}$ m^3/mol (in Ref. 2, $\Delta v_{\beta-\delta} = 1.14 \times 10^{-5}$ m^3/mol is used which corresponds to $\varepsilon^t = 0.07$). The thermodynamic driving force for the $\beta \rightarrow \delta$ PT per unit volume which we will need in the nucleation problem is

$$-\Delta G_{\beta\rightarrow\delta} = -\Delta g_{\beta\rightarrow\delta}\rho/M = [\Delta s_{\beta\rightarrow\delta}(\theta - \theta_e) - p\Delta v_{\beta-\delta}]\rho/M. \tag{4}$$

Similarly, the molar thermodynamic driving force for melting of β and δ phases are

$$-\Delta g_{\beta\rightarrow m} = \Delta s_{\beta\rightarrow m}(\theta - \theta_{m,\beta}) - p\Delta v_{\beta-m} \tag{5}$$

and

$$-\Delta g_{\delta\rightarrow m} = \Delta s_{\delta\rightarrow m}(\theta - \theta_{m,\delta}) - p\Delta v_{\delta-m}. \tag{6}$$

Here $\theta_{m,\beta}$ and $\theta_{m,\delta}$ are the melting temperatures of the β and δ phases at ambient pressure, respectively. The melting temperature of the δ phase reduces with HMX decomposition and that is why it depends on the heating rate. We choose $\theta_{m,\delta} = 550$ K which is within the range given in Refs. 16 and 17 (note that in Refs. 8–10 we used $\theta_{m,\delta} = 551$ K). Taking the enthalpy of melting of the δ phase as $\Delta h_{\delta\rightarrow m} = 69.9$ kJ/(mol K),[2,3] we obtain the entropy of melting of the δ phase $\Delta s_{\delta\rightarrow m} = \Delta h_{\delta\rightarrow m}/\theta_{m,\delta} = 127.09$ J/(mol K). From the temperature independent enthalpy and entropy of these transformations, we obtain the enthalpy and entropy of melting of the β phase: $\Delta h_{\beta\rightarrow m} = \Delta h_{\beta\rightarrow\delta} + \Delta h_{\delta\rightarrow m} = 79.7$ kJ/mol and $\Delta s_{\beta\rightarrow m} = \Delta s_{\beta\rightarrow\delta} + \Delta s_{\delta\rightarrow m} = 149.77$ J/(mol K). The melting temperatures of the β phase are then $\theta_{m,\beta} = \Delta h_{\beta\rightarrow m}/\Delta s_{\beta\rightarrow m} = 532$ K. This is higher than 518.5 K given in Refs. 17 and 20 but is close to our estimate 531.3 K (see Ref. 10, Sec. 4i) based on the extrapolation of the thermodynamic data from Ref. 21. This difference may be related to the inaccuracy of the interpolation of data because of a possible temperature dependence of the transformation enthalphy and entropy; however, it is not important for the current study of the $\beta-\delta$ PT. The change in molar volume during melting of the β and δ phases are: $\Delta v_{\beta-m} = 2.330 \times 10^{-5}$ m^3/mol ($\varepsilon_{\beta-m}^t = 0.147$) and $\Delta v_{\delta-m} = \Delta v_{\beta-m} - \Delta v_{\beta-\delta} = 1.066 \times 10^{-5}$ m^3/mol ($\varepsilon_{\delta-m}^t = 0.067$).[2,3] Since in Ref. 2 we used $\Delta v_{\beta-\delta} = 1.14 \times 10^{-5}$ m^3/mol, $\Delta v_{\delta-m} = 1.19 \times 10^{-5}$ m^3/mol was obtained in that work.

Note that the only independent parameters important for the current study of the $\beta-\delta$ PT (bold in Table I in Ref. 12) are $\Delta h_{\beta\rightarrow\delta} = 9.8$ kJ/mol, $\theta_e = 432$ K, $\Delta h_{\delta\rightarrow m} = 69.9$ kJ/(mol K), $\Delta v_{\beta-\delta} = 1.264 \times 10^{-5}$ m^3/mol, and $\Delta v_{\delta-m} = 1.066 \times 10^{-5}$ m^3/mol, since only they participate in the kinetic equation for the $\beta-\delta$ PT [see Eqs. (16), (19), and (20)]. That is why the uncertainty in other earlier parameters does not affect our results.

The phase equilibrium lines for $\beta-\delta$ PT and the melting of β and δ phases are obtained by setting the driving force to zero. This can be described by the equations

$$p_{\beta-\delta}(\text{MPa}) = -775.139 + 1.794\theta, \tag{7}$$

$$p_{\beta-m}(\text{MPa}) = -3420.600 + 6.428\theta, \tag{8}$$

$$p_{\delta-m}(\text{MPa}) = -6557.22 + 11.922\theta. \tag{9}$$

The pressure-temperature phase equilibrium diagram is presented in Ref. 11. The key point is that with growing pressure the difference in temperature between the $\beta-\delta$ equilibrium and melting of β and δ phases lines reduces. This makes the virtual melting PT mechanism even more probable at high pressure than at ambient pressure. The triple point corresponds to $\theta = 570.224$ and $p = 0.245$ GPa.

III. NUCLEATION MECHANISM FOR THE RECONSTRUCTIVE SOLID-SOLID PHASE TRANSITION IN HMX VIA MELT MEDIATED NANOCLUSTER TRANSFORMATION

A. Experimental observations

We recently observed a paradoxical experimental result:[2,3] the reconstructive $\beta \rightarrow \delta$ PT in HMX starts at 432.6 K, just above the phase equilibrium temperature $\theta_e = 432$ K. Even if θ_e were several degrees lower (for example, due to RDX inclusions), nucleation is still very close to θ_e and all conclusions discussed later would remain valid.

The $\beta \rightarrow \delta$ PT is accompanied by a large volumetric expansion, $\varepsilon^t = 0.08$. Thus, the associated energy of internal stresses ($g^e = 8.947$ kJ/mol, see Ref. 10) is very large and, if not relaxed, should increase the PT temperature by $g^e/\Delta s_{\beta\rightarrow\delta} = 400$ K. The additional nucleation barrier due to the interface energy makes an even larger increase in the nucleation temperature possible. For example, for martensitic PT in steels (which requires deformation only and not reconstruction of the crystal lattice and for which the elastic energy can be easily relaxed through traditional slip and twinning mechanisms, in contrast to HMX), $\varepsilon^t = 0.02$ but the PT onset temperature deviates from θ_e by ~ 100 K. Another example is the PT in KCl which (despite the volume increase of 11%) has a relatively small pressure hysteresis of 0.4 GPa, i.e., the deviation of the transformation pressure from the equilibrium pressure is 0.2 GPa. Using the pressure-temperature equilibrium line for $\beta-\delta$ PT [Eq. (7)], 0.6 K of the deviation of the transformation temperature from the phase equilibrium temperature can be transformed to a pressure deviation of 10^{-3} GPa, which is 200 times smaller than for KCl. No existing theory can explain nucleation so close to the equilibrium line.

The earlier result was obtained for PBX 9501, i.e., for HMX crystals bonded with a binder (Estane and nitroplasticizer). Our preliminary observations in Ref. 22 led us to a hypothesis that β HMX dissolves in the molten nitroplasticizer and at temperatures above θ_e nucleates the δ phase at the interface between the HMX and the liquid.

As we will show later, such a mechanism does completely remove the energy of elastic stresses. We also show

that because of high interface energy any such homogeneous or heterogeneous nucleation is kinetically impossible close to the phase equilibrium temperature. We suggest later that the liquid nitroplasticizer contains nanometer size clusters of the β phase which may appear during dissolution of HMX in the liquid and the destruction of HMX surface asperities. The reconstructive $\beta \rightarrow \delta$ PT in such a cluster is accompanied by a small (or even negative) change in interface energy and allows nucleation of the δ phase near the phase equilibrium temperature. Using this mechanism thermally activated nucleation kinetics is derived.[13] We combine it in Sec. V with our recent results on the virtual melting growth mechanism[8–11] to develop a physically based kinetic model for the $\beta \rightarrow \delta$ PT which is in very good correspondence with our experiments.

B. Nucleation mechanism and kinetics

We first show here that the surface nucleation mechanism discussed earlier[22] completely relaxes the large energy of internal stresses (8.947 kJ/mol) (Ref. 10) that would be generated during direct solid-solid PT. Let nucleation occur in a closed liquid cavity with volume V_l; then the elastic energy due to the volume change is equal to $0.5\ K\varepsilon_0^2$. Here $\varepsilon_0=\varepsilon^t V_n/V_l$ is the volumetric strain in the liquid, V_n is the volume of the δ phase nucleus, and K is the bulk modulus of the liquid. Assuming conservatively the volume of the liquid nitroplasticizer near each HMX crystal $V_l=10^5\times10^5\times10^4=10^{14}$ nm^3 and the volume of nucleus $V_n=10^3$ nm^3 (see our estimates later), we derive $\varepsilon_0=10^{-11}\varepsilon^t=8\times10^{-13}$, which is negligible. Because in reality volume V_l is not closed, volumetric strain ε_0 is even smaller.

1. Impossibility of a classical homogeneous and heterogeneous nucleation

Despite the relaxation of internal stresses, the nucleation barrier due to the interface energy is still too large to allow such a nucleation mechanism close to the phase equilibrium temperature. The time for a thermally activated nucleation is described by the Arrhenius equation[23,24]

$$t_n=\tilde{t}\frac{h}{k\theta}\exp\left(\frac{E_n}{k\theta}\right)=\frac{\bar{t}}{\theta}\exp\left(\frac{E_n}{k\theta}\right), \tag{10}$$

where $k=1.381\times10^{-23}$ J/K and $h=6.626\times10^{-34}$ J s are Boltzmann's and Planck's constants, E_n is the activation energy for nucleation, and $\bar{t}$ and $\tilde{t}$ are pre-exponential multipliers (determined later from the best fit to experimental data). The activation energy is equal to the energy of a critical nucleus. For a spherical nucleus it is described by the well known equation[23]

$$E_n=\frac{16\pi\Delta\gamma^3}{3\Delta G_{\beta\rightarrow\delta}^2}, \tag{11}$$

where $\Delta\gamma$ is the change in surface energy. For precipitation of the δ phase from the solution of HMX in liquid nitroplasticizer, $\Delta G_{\beta\rightarrow\delta}$ has to take into account the thermodynamic properties of solution. They are unknown, so we will use the difference in the Gibbs potential of the β and δ phases, which as we will see does not change our conclusions. Substituting $\Delta G_{\beta\rightarrow\delta}$ and all the earlier data in Eq. (11), one obtains for $p=0$,

$$E_n=\frac{8.366\times10^{-10}\Delta\gamma^3}{(\theta-432)^2}. \tag{12}$$

Nucleation can occur during the time of an experiment only if $E_n=40k$ to $80k\theta$.[23] Indeed, for $E_n=40$ to $80k\theta$, $\exp(E_n/k\theta)=10^{17}-10^{34}$. For $\bar{t}/\theta=10^{-17}$ s (which has the meaning of the nucleation time for $E_n=0$), Eq. (10) results in nucleation time $t_n=(1-10^{17})$ s that can be realized in experiments or in nature. On the other hand, for $\gamma_{s-l}=6\times10^{-2}$ J/m^2 and $\theta=432.6$ K, we obtain from Eq. (10) $t_n=10^{36489442}$ s; for $\gamma_{s-l}=10^{-2}$ J/m^2 and $\theta=438$ K (which increases $\Delta G_{\beta\rightarrow\delta}$ by a factor of 10), we still have $t_n=10^{1646}$ s, which is absolutely unrealistic for an actual nucleation.

Taking $\theta=432.6$ K and $E_n=80k\theta$, we estimate from Eq. (12) the change in surface energy of $\Delta\gamma<6\times10^{-4}$ J/m^2 that allows the nucleation. This number is extremely small in comparison with reality. For homogeneous nucleation of δ crystals in the molten nitroplasticizer, $\Delta\gamma$ is the interface energy between the solid δ phase and liquid nitroplasticizer, $\gamma_{\delta-l}$. Usually the solid-liquid interface energy is of the order of magnitude $\gamma_{s-l}=10^{-1}-10^{-2}$ J/m^2. Consequently, homogeneous nucleation is impossible, like for most PTs. Assuming $\gamma_{s-l}=6\times10^{-2}$ J/m^2, then the activation energy for homogeneous nucleation is six orders of magnitude larger than allowable by the equation $E_n=80k\theta$. Even for $\gamma_{s-l}=10^{-2}$ J/m^2, an eventual increase in the driving force for a PT by one order of magnitude, due to the temperature dependence in $-\Delta G_{\beta\rightarrow\delta}$, by an eventual chemical reaction, or by the thermodynamics of dissolution of HMX in the liquid phase, does not change our conclusion that the homogeneous nucleation is impossible.

For heterogeneous nucleation at the flat surface of the β phase one obtains[23]

$$E_n=\frac{8.366\times10^{-10}\gamma_{\delta-l}^3}{(\theta-432)^2}S(\alpha),$$

$$S(\alpha):=(2+\cos\alpha)(1-\cos\alpha)^2/4. \tag{13}$$

Here the wetting angle α is determined by the mechanical equilibrium of the components of surface tension along the flat interface,[23] namely $\gamma_{\beta-l}=\gamma_{\beta-\delta}+\gamma_{\delta-l}\cos\alpha$ [i.e., $\cos\alpha=(\gamma_{\beta-l}-\gamma_{\beta-\delta})/\gamma_{\delta-l}$], where $\gamma_{\beta-l}$ is the energy of interfaces between the β phase and surrounding liquid and $\gamma_{\beta-\delta}$ is the $\beta-\delta$ interface energy. A low-energy coherent interface between the β and δ phases cannot be expected because it will cause a significant increase in elastic energy of internal stresses and create an additional thermodynamic barrier to nucleation. Usual estimates for an incoherent interface are $\gamma_{\beta-\delta}\simeq1$ J/m$^2\simeq10\gamma_{s-l}$ to $100\gamma_{s-l}$. Heterogeneous nucleation is favorable in comparison with the homogeneous one for $\cos\alpha\simeq1$, i.e., for $\gamma_{\beta-l}\gg\gamma_{\beta-\delta}$. In fact, our case is the opposite, i.e., $\gamma_{\beta-l}\ll\gamma_{\beta-\delta}$. For such a situation, the mechanical equilibrium $\gamma_{\beta-l}=\gamma_{\beta-\delta}+\gamma_{\delta-l}\cos\alpha$ is not satisfied and wetting is impossible. Thus, heterogeneous nucleation at the in-

terface between the liquid and the β phase is kinetically even less favorable than homogeneous nucleation.

2. Nucleation mechanism via cluster to cluster transformation

Let us consider the following mechanism of $\beta \rightarrow \delta$ PT through a liquid nitroplasticizer. We assume that the liquid medium contains nanometer size clusters of the β phase that may appear during destruction of HMX surface asperities and their suspension in the liquid. When such a cluster undergoes the reconstructive $\beta \rightarrow \delta$ PT, then the activation energy for nucleation is determined by the same Eq. (11) [or Eq. (12)] but with different change in surface energy, $\Delta\gamma = \gamma_{\delta-l} - \gamma_{\beta-l}$. Both $\gamma_{\delta-l}$ and $\gamma_{\beta-l}$ are large but are of the same order of magnitude. Then their difference, $\gamma_{\delta-l} - \gamma_{\beta-l}$, can be much smaller than each of them ($\gamma_{\delta-l}$ or $\gamma_{\beta-l}$), i.e., it can be as small as $(4.7-5.9)10^{-4}$ J/m^2 required by the kinetic nucleation condition $E_n = 40$ to $80k\theta$,[23] or even smaller. Moreover, for one of the PTs, $\beta \rightarrow \delta$ or $\delta \rightarrow \beta$, the change in interface energy $\Delta\gamma$ is negative because they differ by a sign only. This means that the barrierless nucleation of the δ (or β) phase may occur in the β (or δ) cluster. The radius of the critical cluster is determined by the well known equation[23]

$$r_c = \frac{2\Delta\gamma}{\Delta G_{\beta\rightarrow\delta}} = 1.4 \times 10^{-5} \frac{\Delta\gamma}{(\theta - 432)}. \tag{14}$$

For $\theta = 432.6$ and $\Delta\gamma = 4.78 \times 10^{-4}$ J/m^2 (the value that will be obtained later), we calculate the radius of $r_c = 11$ nm; a decrease in change of the interface energy $\Delta\gamma$ or increase in the deviation from the phase equilibrium temperature, $\theta - 432$, reduces the cluster radius proportionally.

The region near the interface between the β phase and nitroplasticizer is the most probable place where a critical δ phase cluster may nucleate. The nucleus can grow via dissolution of the surface of the β phase crystal, diffusion of molecules through nitroplasticizer toward the growing δ crystal, and subsequent crystallization onto the surface of the stable δ cluster. The observable macroscopic growth kinetics will only be determined by those nuclei from the entire population of supercritical nuclei (that are usually called operational nuclei) that are close enough to the interface with the β phase and have the smallest diffusion path. Some δ crystals may touch the β crystal surface (in particular, due to gravitational and/or electrostatic forces) and form a new $\beta - \delta$ interface. This interface initially contains a very thin layer of nitroplasticizer; when the interface area grows due to the $\beta \rightarrow \delta$ PT, content of the nitroplasticizer in the interface is negligible. Thus, the suggested melt mediated cluster to cluster PT nucleation mechanism completely relaxes the elastic energy of internal stresses and reduces by orders of magnitude the change in interfacial energy. That is why it makes possible nucleation very close to the phase equilibrium temperature and it initiates the virtual melting mechanism of growth in the bulk by contact of δ clusters with the β surface phase of larger crystals. This mechanism will be further elaborated and used later for the development a fully physical overall kinetic model for the $\beta \rightarrow \delta$ PT.

IV. GROWTH MECHANISM AND KINETICS FOR $\beta \leftrightarrow \delta$ PHASE TRANSFORMATION IN HMX VIA VIRTUAL MELTING

A. Virtual melting growth mechanism

During the solid-solid PT, the transformation strain may generate two types of internal elastic stresses:

(a) Due to the displacement continuity across a coherent interface. If the interface completely (or partially) loses its coherence, theses stresses completely (or partially) relax.

(b) Due to a change in volume during the PT if the δ phase is completely embedded inside the β phase. Even loss of interface coherence does not relax these stresses.

The energy of the internal stresses increases the PT temperature. However, since nucleation and growth of the δ phase in PBX 9501 starts at the surface of the β crystal, the type (b) of internal stresses can be neglected. They are important, however, for the PT in crystalline HMX without the binder where the PT starts inside the crystal at some nucleation sites.

We demonstrated earlier[8–10] that the energy of the internal stresses of type (a) at the initially coherent $\beta - \delta$ interface ($g^e = 8.947$ kJ/mol) is sufficient to make the energy of the stressed layer of the δ phase equal to the energy of the melt. Thus, it melts approximately 120 K below the normal melting temperature of the δ phase, $\theta_{m,\delta} = 550$ K, i.e., around the $\beta - \delta$ phase equilibrium temperature of $\theta_e = 432$ K at ambient pressure during the $\beta \rightarrow \delta$ PT. It is also sufficient to reduce the melting temperature of the β phase from 520 to 400 K for the β phase during the $\delta \rightarrow \beta$ PT. Melting of the thin layer is accompanied by a decrease in the interface energies, i.e., the melt nucleation is barrierless.[8,10] After melting, the elastic stresses completely relax and the interface completely loses its coherence. A stress-free melt is unstable with respect to stable δ phase and it solidifies into the δ phase. The melt in each transforming material point exists during an extremely short time required for stress relaxation. We called it the virtual melt, because it represents a transitional activated state rather than a thermodynamically stable melt.

A volume decrease during solidification results in tensile stresses in the solidifying layer of the δ phase. Since resistance to fracture during solidification is negligible, the elastic strains completely relax through nanocracking, vacancy, and void generation. This explains the nanoporosity that was observed in experiments in Refs. 2 and 3. Without the virtual melting, compressive stresses caused by the expansion of the δ phase could not lead to nanocracking. The nanoporosity during the solidification is generated when stresses are near zero and that is why it does not change the thermodynamics and kinetics of the $\beta \rightarrow \delta$ PT; the virtual melting eliminates the whole thermomechanical memory of preceding cycles of the $\beta \leftrightarrow \delta$ PT.[8–10] These results explain the paradoxical independence of the thermodynamics and kinetics for the first and the second direct-reverse transformation cycles that was observed in experiments in Refs. 2 and 3. Under high external pressure, we assume that porosity will be closed immediately after its appearance because the yield stress is close to

zero. Thus, we neglect the damage during the $\beta \rightarrow \delta$ PT via virtual melting. Also, the athermal interface friction K_{at} disappears for the virtual melting growth mechanism because the melt as a hydrostatic medium does not interact with the long range stress field of the crystal lattice defects.[8–10] This explains why the transformation can progress under a surprisingly small thermodynamic driving force. For the other PTs in the HMX system, like $\alpha \leftrightarrow \delta$ and $\alpha \leftrightarrow \beta$, the change in volume is approximately two times smaller and cannot cause melting. This unrelaxed elastic energy and athermal interface friction explains the relatively large temperature hysteresis observed in these systems. In total, 16 theoretical predictions are in qualitative and quantitative correspondence with experiments performed on the PTs in the HMX energetic crystal.

B. Growth kinetics

The velocity of the $\beta-\delta$ phase interface can be described by the thermally activated kinetics[8] utilizing the virtual melting mechanism

$$v = \bar{v}_0 \left[\exp\left(-\frac{g_{\beta\rightarrow m}}{R\theta} \right) - \exp\left(-\frac{g_{\delta\rightarrow m}}{R\theta} \right) \right] = \bar{v}_0 \exp\left(-\frac{g_{\delta\rightarrow m}}{R\theta} \right) \left[\exp\left(-\frac{g_{\beta\rightarrow\delta}}{R\theta} \right) - 1 \right], \tag{15}$$

where $\bar{v}_0$ is the pre-exponential factor. Since

$$\begin{aligned} &\bar{v}_0 \exp(-g_{\delta\rightarrow m}/R\theta) \\ &= \bar{v}_0 \exp[-(\Delta h_{\delta\rightarrow m} - \theta \Delta s_{\delta\rightarrow m} + p\Delta v_{\delta\rightarrow m})/R\theta] \\ &= \bar{v}_0 \exp(\Delta s_{\delta\rightarrow m}/R) \exp[-(\Delta h_{\delta\rightarrow m} + p\Delta v_{\delta\rightarrow m})/R\theta] \\ &= v_0 \exp[-(\Delta h_{\delta\rightarrow m} + p\Delta v_{\delta\rightarrow m})/R\theta], \end{aligned}$$

where $v_0 = \bar{v}_0 \exp(\Delta s_{\delta\rightarrow m}/R)$, then

$$v = v_0 \exp\left(-\frac{\Delta h_{\delta\rightarrow m} + p\Delta v_{\delta-m}}{R\theta} \right) \left[\exp\left(-\frac{\Delta g_{\beta\rightarrow\delta}}{R\theta} \right) - 1 \right], \tag{16}$$

where v_0 was found in Refs. 9 and 10 to be 10^{10} μm/s $= 10^4$ m/s. The term in square parenthesis is a function of the driving force for $\beta \rightarrow \delta$ PT, which is equal to zero for thermodynamic equilibrium and greater (smaller) than zero in the region of stability of the δ (β) phase; Eq. (16) is valid for both $\beta \rightarrow \delta$ (for $v > 0$) and $\delta \rightarrow \beta$ (for $v < 0$) PT. The temperature dependence of the rate constant is determined by the heat of fusion $h_{\delta\rightarrow m}$ and transformation work of fusion $p\Delta v_{\delta-m}$. Predictions of Eq. (16) are in a good agreement with various experiments under ambient pressure, see Refs. 9–11. The time derivative of the volume fraction of the δ phase due to interface motion, $\dot{c}_g$, can be determined by the approximate equation

$$\dot{c}_g = \int_\Sigma v d\Sigma / V = v_{av} \Sigma / V, \tag{17}$$

where V is the volume of the crystal, Σ is the total area of the $\beta-\delta$ interface, and v_{av} is the averaged interface velocity over the area Σ. The total area of interfaces is a function of the propagation geometry. For the case with numerous interfaces of stochastic geometry, the approximation $\Sigma \sim c(1-c)$ can be used. The last equation at least satisfies two limiting cases of zero area at the beginning and end of PT. If we consider a group of HMX crystals and in each of them there is a single interface, but the interface geometry in each crystal is different, then the interface area Σ averaged over the group of crystals is similar to that for a single crystal with a stochastic interface geometry, i.e., $\Sigma \sim c(1-c)$. Assuming that v_{av} can be determined by Eq. (16), one obtains

$$\dot{c}_g = Bvc(1-c) = \bar{c}_g c(1-c) \exp\left(-\frac{\Delta h_{\delta\rightarrow m} + p\Delta v_{\delta-m}}{R\theta} \right) \times \left[\exp\left(-\frac{\Delta g_{\beta\rightarrow\delta}}{R\theta} \right) - 1 \right]. \tag{18}$$

Here B and $\bar{c}_g$ are the parameters that will be found from experiments. According to transition state theory,[24] we assume (similar to nucleation) $\bar{c}_g = Z(k\theta/h)$, where Z is the parameter that will be determined from the best fit to experiments.

V. OVERALL KINETICS OF $\beta \leftrightarrow \Delta$ PHASE TRANSFORMATION IN HMX

The overall nucleation and growth kinetics is described by the kinetic growth Eq. (18) supplemented by the nucleation-motivated initial condition

$$\dot{c} = bc(1-c); \quad c(t_0) = c_0, \tag{19}$$

$$b := Z\frac{k\theta}{h} \exp\left(-\frac{\Delta h_{\delta\rightarrow m} + p\Delta v_{\delta-m}}{R\theta} \right) \left[\exp\left(-\frac{\Delta g_{\beta\rightarrow\delta}}{R\theta} \right) - 1 \right]. \tag{20}$$

We need to distinguish between a critical nucleus, i.e., a nucleus that corresponds to a maximum of Gibbs energy and has equal probability to grow or disappear, and an operational nucleus, i.e., a nucleus which cannot disappear and for which the volume fraction c_0 that is reached at time t_0 can be used as an initial condition in the overall macroscopic kinetic equation. There are a number of unknown parameters, like the diffusion coefficient and path, rate of dissolution and crystallization, which do not allow us to describe in detail the diffusional growth of a critical nucleus to the operational one. That is why we assume in the first approximation that t_0 is proportional to t_n, i.e., from Eq. (10),

$$t_0 = \frac{\bar{t}_0}{\theta} \exp\left(\frac{E_n}{k\theta} \right) = \frac{\bar{t}_0}{\theta} \exp\left(\frac{16\pi\Delta\gamma^3}{3\Delta G^2_{\beta\rightarrow\delta} k\theta} \right), \tag{21}$$

where $\bar{t}_0$ is the pre-exponential factor. We also assume that the volume fraction of an operational nucleus c_0 is a constant. For ambient pressure, Eq. (21) simplifies to

$$t_0 = \frac{\bar{t}_0}{\theta} \exp\left[\frac{6.058 \times 10^{13} \Delta\gamma^3}{(\theta - 432)^2 \theta} \right]. \tag{22}$$

The analytical solution to Eq. (19) under constant temperature and pressure is as follows:

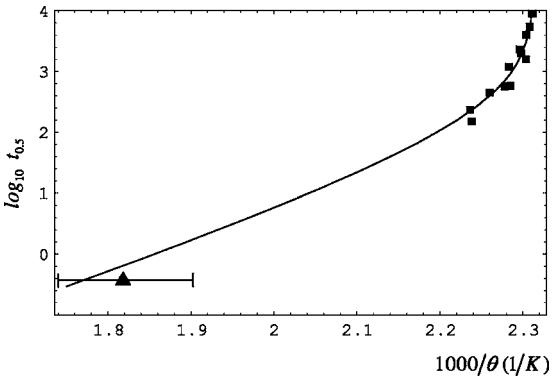

FIG. 1. A comparison of the predictions of Eq. (24) (solid line) with experimental data. The logarithm of the time to half conversion vs $1000/\theta(K)$ for $\beta\rightarrow\delta$ PT in the HMX based plastic bonded explosive PBX 9501. Squares are data from measurements made by second harmonic generation (Refs. 2 and 3); the triangle is the conversion half time measured during laser heating (Ref. 25).

$$c=\frac{c_0}{c_0+(1-c_0)\exp[-b(t-t_0)]}. \tag{23}$$

For $c=0.5$ one can find the time to half conversion which was used in Refs. 2–4 to compare with experiment. This leads to

$$t_{0.5}=t_0+\frac{\ln\left(\frac{1}{c_0}-1\right)}{b}. \tag{24}$$

More generally, the time to reach the volume fraction f can be found from the condition $c=f$,

$$t_f=t_0+\frac{\ln\left[\frac{(1-c_0)f}{c_0(1-f)}\right]}{b}. \tag{25}$$

Thus, the time to reach any volume fraction f consists of the time for appearance of an operational nucleus t_0 and time for its growth.

A. Parameter identification and comparison with experiments

Substituting into Eq. (24) for the time to half conversion, Eq. (22) for nucleation time t_0 and Eq. (20) for the coefficient b, we obtain that $t_{0.5}$ depends on three material parameters: $\Delta\gamma$, $\bar{t}_0$, and $\bar{Q}=\ln(1/c_0-1)/Z$.

In Fig. 1, a good agreement between the prediction of Eq. (24) and the experimental data for $t_{0.5}$ for $\beta\rightarrow\delta$ transformation[2,3] was obtained. Parameters $\Delta\gamma=4.78\times10^{-4}$ J/m^2, $\bar{t}_0=4.5\times10^{-4}$ s, and $\bar{Q}=5.822\times10^{12}$ are determined from the best fit to experiments for the time to half conversion. Even extrapolation of our equation for $\theta=550$ K, where our nucleation and growth mechanisms may not be operative, gives good agreement (Fig. 1) with a laser heating experiment.[25] Parameters Z and c_0 can be varied in order to achieve the best correspondence between predicted and experimental shape of the $c(t)$ curves. However, this degree of freedom is not necessary. We did not change our virtual melting based growth model[11] and retain the value of the parameter $Z=7\times10^{-13}$; that gives us $c_0=0.016$ for the

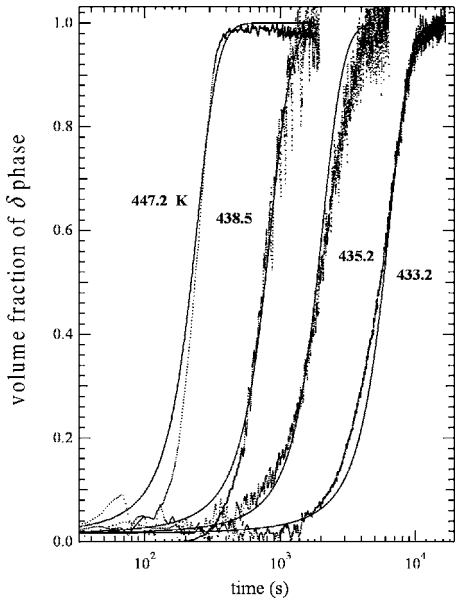

FIG. 2. A comparison between prediction of Eq. (23) (solid curves) with experimental data for $\beta\rightarrow\delta$ PT in the HMX based plastic bonded explosive PBX 9501 (Refs. 2 and 3) under isothermal conditions. The volume fraction of the δ phase c is equal to square root of the measured second harmonic generation intensity from the HMX δ phase. The zero of time is the point at which the heated sample reached the labeled isothermal temperature.

concentration of the operational nucleus. All kinetic parameters are summarized in Table II in Ref. 12. Figure 2 exhibits a very good correspondence between kinetic curves predicted by Eq. (23) and experiment. Note that extrapolation to a wider range of parameters (pressure and temperature) is much more reliable for the present physical model than for the phenomenological model in Ref. 11 (see Sec. IV in Ref. 12).

Note that for diffusional PTs $\bar{t}_0/\theta$ in Eq. (22) has to be presented in the form $\hat{t}\exp(Q_{sd}/k\theta)$, where Q_{sd} is the activation energy of self-diffusion[23] [the same is valid for Eq. (10)]. However, this does not change our model because of the much stronger temperature dependence of t_0 due to E_n. In the narrow temperature range where t_0 is greater than or comparable with propagation time, both equations give very close results. At higher temperatures, t_0 is negligible in Eq. (24). That is also why we are unable to determine Q_{sd} with reasonable accuracy.

B. Nucleation under variable temperature and pressure

If temperature and pressure are variable, the nucleation time t_0 has to be evaluated starting with the instant when the PT criterion is met. Since we will consider only relatively slow loading and changes in temperature and pressure that are small during the nucleation time, we will use Eq. (21) substituting in it the values of temperature and pressure at time t_0, i.e., $\theta(t_0)$ and $p(t_0,c_0)$,

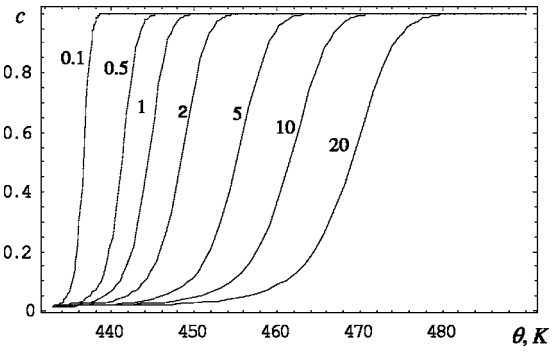

FIG. 3. Evolution of the volume fraction of the δ phase based on solution of Eqs. (19), (20), and (27) under zero pressure and various heating rates (shown in K/min near the curves).

$$t_0 = \frac{\bar{t}_0}{\theta(t_0)} \times \exp\left(\frac{16\pi M^2 \Delta\gamma^3}{3\{\Delta s_{\beta\to\delta}[\theta(t_0) - \theta_e] - p(t_0, c_0)\Delta v_{\beta-\delta}\}^2 \rho_h^2 k \theta(t_0)} \right). \tag{26}$$

This nonlinear algebraic equation has to be solved numerically for t_0. Note that the appearance of operational nuclei with $c_0=0.016$ causes an instantaneous pressure change. This has to be defined from the solution of the mechanical problem and taken into account in $p(t_0, c_0)$ in Eq. (26).

In the problem considered in Sec. VII and in Ref. 12 a constant temperature rate, h_r, is prescribed and pressure, $p(\theta)$, is determined as a function of θ from the solution of the mechanical problem. First, the mechanical problem without PT is solved and temperature θ_i at which PT criterion is met is determined from the nonlinear equation $\Delta s_{\beta\to\delta}(\theta_i - \theta_e) = p(\theta_i)\Delta v_{\beta-\delta}$. Since $\varepsilon_b^m = \varepsilon_N^m$, we can express time in terms of θ, i.e., $t=(\theta-\theta_i)/h_r$ and use temperature as an independent variable. Then introducing the constant $c=c_0$ in the mechanical problem and expressing the solution $p(t, c_0)$ in terms of temperature, we can determine the nucleation temperature, θ_0, from the equation

$$\frac{\theta_0 - \theta_i}{h_r} = \frac{\bar{t}_0}{\theta_0} \times \exp\left\{ \frac{16\pi M^2 \Delta\gamma^3}{3[\Delta s_{\beta\to\delta}(\theta_0 - \theta_e) - p(\theta_0, c_0)\Delta v_{\beta-\delta}]^2 \rho_h^2 k \theta_0} \right\}. \tag{27}$$

Kinetic curves for the $\beta\to\delta$ PT for zero pressure and various heating rates are shown in Fig. 3. Note that the nucleation temperature varies in a very narrow range from 432.86 K for $h_r=0.1$ K/min to 433.0 K for $h_r=20$ K/min. Despite the fact that the nucleation time at isothermal conditions of 432.86 K is 566 s and at 433.0 K is 3 s, multiplication of each of these times by the corresponding heating rate gives approximately the same temperature increment of 1 K. Thus, the main difference in the kinetic curves for different heating rates is due to the temperature dependence of the growth stage.

VI. CONTINUUM MECHANICAL MODEL FOR A COMPOSITE CONSISTING OF CRYSTALLINE HMX EMBEDDED IN A BINDER AND ALLOWING FOR PHASE TRANSFORMATION AND CHEMICAL DECOMPOSITION

The PBX 9501 formulation consists of HMX and binder. The binder consists of Estane and nitroplasticizer (equal masses) as well as of 0.1% of an antioxidant (which we will neglect). The initial mass fraction of HMX, nitroplasticizer, and Estane are $\phi_{0h}=0.95$, $\phi_{0N}=0.025$, and $\phi_{0E}=0.025$, respectively. In designations of the concentrations of various components, we will use ϕ for mass fractions and f for volume fractions. No extra subscripts will be used for volume fractions with respect to void-free PBX, a subscript "v" will be utilized for volume fractions with respect to PBX with voids and a subscript "0" for a initial value. The mass densities of HMX, nitroplasticizer, and Estane are $\rho_h = 1905$ kg/m^3, $\rho_N=1390$ kg/m^3, and $\rho_E=1190$ kg/m^3, respectively. The mass density of any composite can be determined by the equation $\rho=(\sum_i f_i/\rho_i)^{-1}$. Thus, the mass density of the binder and void-free PBX are $\rho_b=1282$ kg/m^3 and $\rho_P=1860$ kg/m^3. The mass density of PBX containing a volume fraction f_v of voids (with respect to total PBX plus void volume) is $\rho_{Pv}=\rho_P(1-f_v)$ and is equal to 1832 -1823 kg/m^3 for $f_v=0.015-0.02$. The volume fractions of components with respect to a void free material can be determined by equation

$$f_k = \phi_k \rho_P/\rho_k, \quad k=1,2,3, \tag{28}$$

and are equal initially to $f_{0h}=0.928$, $f_{0N}=0.033$, $f_{0E}=0.039$, and $f_{0b=}f_{0N}+f_{0E}=0.072$ for HMX, nitroplasticizer, Estane, and binder. Adding a volume fraction of voids, f_v, changes the volume fraction with respect to porous material to

$$f_{kv} = f_k(1-f_v), \quad k=1,2,3. \tag{29}$$

Summation of all f_{kv} gives $1-f_v$. For example, for initial $f_{0v}=0.015$ we obtain $f_{0hv}=0.913$, $f_{0Nv}=0.033$, and $f_{0Ev}=0.039$. The melting temperature of Estane is 350 K and the melting temperature of nitroplasticizer is $\sim$377 K. In the temperature range of PT ($\theta>432$ K), the shear modulus of the binder, μ_b, has to be equal to zero; however, for generality, we will first consider a small but nonzero μ_b. Also, nitroplasticizer decomposes and disappears with time in the temperature range of 360–520 K (heating rate 0.5 -10 K/min) and Estane decomposes and disappears at temperature above 520 K. HMX decomposes at temperature above 453 K.

A. Geometrically linear theory

In the process of PT in HMX and chemical decomposition of the binder, finite ($\sim$0.1) and large ($\gg$0.1) strains are involved. In particular, transformation plus thermal strain in HMX may reach 0.1 and strain due to mass loss of the nitroplasticizer may reach 0.5. Thus, a geometrically nonlinear theory is necessary. We will approach this problem in two steps. First, we show based on geometrically linear theory that the effect of the shear modulus of the binder and internal stresses between the HMX and the binder can be neglected,

i.e., the composite can be considered as a hydrostatic medium. This simplification allows us to develop an exact geometrically nonlinear theory.

The effective bulk modulus of the composite, K_c, can be determined using the methods described in Ref. 26. In particular, both polydisperse and three phase models give the same expression

$$K_c = K_b + \frac{f(K_h - K_b)}{1 + \frac{(1-f)(K_h-K_b)}{K_b+4\mu_b/3}}, \tag{30}$$

where K_h and K_b are the bulk moduli of HMX crystal and binder and f is the volume fraction of the HMX crystals; voids are included in inelastic damage strains. If we decompose this expression in a Taylor series in μ_b, then the second term is proportional to $(1-f)\mu_b$, i.e., is negligible due to small $(1-f)$ and μ_b. The first term is

$$K_c = \left(\frac{f}{K_h} + \frac{1-f}{K_b}\right)^{-1}, \tag{31}$$

which corresponds to a volume averaging of the bulk compliances (the Reuss scheme).

To find a pressure-volume relationship for the composite and pressure in HMX crystals (which we need to use in the PT kinetics) we will use the following simple model: a spherical inclusion of radius r of HMX crystal within a spherical layer of the binder (external radius r_e) under external pressure p, $f=(r/r_e)^3$. Because of the small shear modulus and concentration of the binder, it acts almost like a liquid and the specific shape is not important. The pressure p-volumetric strain ε relations for each phase are assumed to be in the form of Hooke's law

$$p_h = -K_h(\varepsilon_h - \varepsilon_h^i), \quad p_b = -K_b(\varepsilon_b - \varepsilon_b^i), \tag{32}$$

where ε_h^i and ε_b^i are inelastic deformations in the HMX and the binder which include thermal, transformational, and damage (due to porosity) parts. The minus sign in Eq. (32) is used because we consider the tensile strains and compressive pressure as positive. Taking into account the continuity of displacements and radial stresses across the HMX-binder interface and borrowing the well-known solution of the corresponding elastic problem (see e.g., Ref. 27), we obtain

$$p_h = pK_h(3K_b + 4\mu_b)/L + 4(\varepsilon_h^i - \varepsilon_b^i)(1-f)K_hK_b\mu_b/L, \tag{33}$$

$$\varepsilon = -p(3(1-f)K_h + 3fK_b + 4\mu_b)/L + (\varepsilon_b^i(1-f) \times K_b(3K_h + 4\mu_b) + \varepsilon_h^i fK_h(3K_b + 4\mu_b))/L,$$

$$L := 4f(K_h - K_b)\mu_b + K_b(4\mu_b + 3K_h). \tag{34}$$

In Eq. (33) pressure in the HMX crystal consists of terms proportional to the external pressure and internal stresses. Although the jump in strain due to PT in HMX $\varepsilon_{hi}-\varepsilon_{bi}$ is large ($\sim$0.08), multiplication by two small terms $(1-f)\mu_b$ makes the internal stresses negligible. Using the Taylor series in μ_b for the first term results in

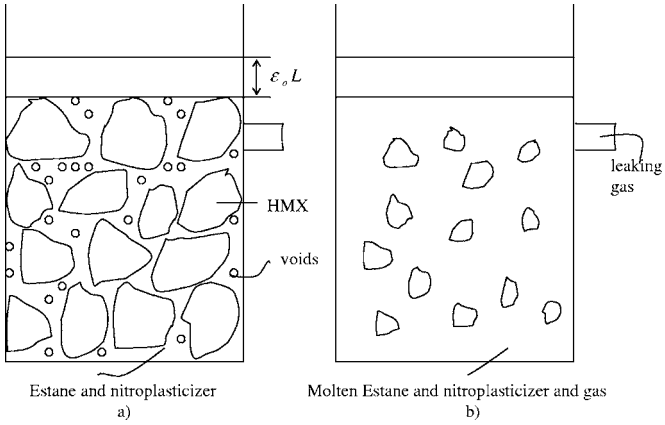

FIG. 4. Scheme of the PBX formulation heated in a rigid cylinder (a) in initial state and (b) during the heating and occurring all thermomechanochemical processes. It is assumed that the molten binder fills immediately all voids. HMX crystals are under hydrostatic pressure imposed by the molten Estane and nitroplasticizer and gas.

$$p_h = p\left[1 + \frac{4(K_h - K_b)(1-f)\mu_b}{3K_hK_b}\right], \tag{35}$$

where the second term is again negligible due to small $(1-f)\mu_b$. Thus, $p_h=p$ is a good approximation even for small but nonzero $(1-f)\mu_b$. This means that when the external pressure is prescribed, the thermodynamics and kinetics of $\beta \rightarrow \delta$ PT in PBX 9501 can be considered using the applied pressure p, like for HMX crystals without a binder. Expanding Eq. (34) in a Taylor series in μ_b, one obtains

$$\varepsilon = -p\left[\left(\frac{f}{K_h} + \frac{1-f}{K_b}\right) - \frac{4(K_h - K_b)^2 f(1-f)\mu_b}{3K_h^2K_b^2}\right] + [f\varepsilon_h^i + (1-f)\varepsilon_b^i] + \frac{4(\varepsilon_h^i - \varepsilon_b^i)(K_h - K_b)f(1-f)\mu_b}{3K_hK_b}. \tag{36}$$

Neglecting the terms with $(1-f)\mu_b$ results in a final expression

$$\varepsilon = -p\left(\frac{f}{K_h} + \frac{1-f}{K_b}\right) + [f\varepsilon_h^i + (1-f)\varepsilon_b^i] \tag{37}$$

with simple volume averaging of bulk compliances and inelastic strains.

B. Geometrically nonlinear theory

We will now consider the following problem (Fig. 4). Let the cylindrical PBX sample be placed into a rigid cylinder and an initial macroscopic compressive strain ε_0 be prescribed by the piston motion. Then the sample is homogeneously heated with the heating rate h_r during which ε_0 is kept constant. Pressure increases due to the thermal expansion. In the temperature range 350–370 K, the nitroplasticizer and Estane melt. All initial voids are filled immediately by the binder as soon as it melts and any external pressure is applied. The mass of the gas in the initial voids will be neglected. We will determine the pressure change and its effect on the $\beta \rightarrow \delta$ PT after the melting of the binder only. We will consider the simultaneous occurrence of the $\beta \rightarrow \delta$

PT and chemical decomposition of the nitroplasticizer and HMX. The gas which appears due to the binder and HMX decomposition partially disappears due to the leaking from the cylinder and partially remains as a new phase. It fills the voids that are created by decomposition of the binder and HMX and the initial voids that may still be left after melting of the binder and thermal expansion. We will neglect the closed voids inside the HMX that are not accessible by the molten binder or gas.

We neglect the nonhydrostatic stresses in the binder and the resulting hydrostatic stresses in HMX crystals embedded in the binder. Since pressure and temperature are homogeneous, the problem of developing a constitutive model for the PBX and consideration of deformation of the PBX in the cylinder are the same. The main challenge is to correctly take into account the large deformations due to chemical decomposition of the binder and HMX and change in gas volume, as well as finite elastic deformation of the binder and the transformation and thermal strain in the HMX. Special attention has to be paid to the large strain due to chemical decomposition in the binder and HMX and the change in gas volume because they also change the mass and volume fraction of the phases. Also, the large elastic strain of the binder and transformation strain of the HMX change the volume fraction of the phases. All these points have to be carefully taken into account by a strict geometrically nonlinear (large strain) formulation. A general geometrically nonlinear kinematic approach to the thermomechanical processes with several strain components can be found in Refs. 28 and 29. We will generalize them for the case with mass loss and specify them for the pure volumetric strain.

Let us consider volumetric strains of crystalline HMX under applied pressure and heating when accompanied by PT, chemical decomposition, thermal, and elastic stresses. If the initial stress-free volume at initial temperature $\theta_{\text{in}}=300$ K is V_h^0 (the subscript h designates HMX) and the volume at some instant t of thermomechanical loading is V_h, we can define the volumetric deformation gradient (one dimensional) $F_h=V_h/V_h^0$ and volumetric strain $\varepsilon_h=F_h-1$. We can introduce components of the deformation gradient: $F_h^m=V_h^m/V_h^0$ due to the mass loss during the chemical decomposition, where V_h^m is the stress-free volume at temperature θ_{in} after the mass loss at time t; the transformation deformation gradient $F_h^t=V_h^t/V_h^m=1.08$ which transforms the volume V_h^m of the β phase to the volume V_h^t of the δ phase; the thermal deformation gradient $F_h^\theta=V_h^\theta/V_h^t$, where V_h^θ is the stress-free volume at current temperature θ; and the elastic deformation gradient $F_h^e=V_h/V_h^\theta$ which characterizes the elastic deformation due to external pressure. Each strain component is determined through the corresponding deformation gradient using the same equation as for the total strain

$$\varepsilon_h^m=F_h^m-1,\quad \varepsilon_h^t=F_h^t-1,\quad \varepsilon_h^\theta=F_h^\theta-1,\quad \varepsilon_h^e=F_h^e-1. \tag{38}$$

Since

$$F_h=\frac{V_h}{V_h^0}=\frac{V_h}{V_h^\theta}\frac{V_h^\theta}{V_h^t}\frac{V_h^t}{V_h^m}\frac{V_h^m}{V_h^0}, \tag{39}$$

one obtains the multiplicative decomposition

$$F_h=F_h^eF_h^\theta F_h^tF_h^m. \tag{40}$$

Note that in one dimension the sequence of the terms in Eq. (40) is not important. Substituting expressions for deformation gradients in terms of corresponding strains, we have

$$1+\varepsilon_h=(1+\varepsilon_h^e)(1+\varepsilon_h^\theta)(1+\varepsilon_h^t)(1+\varepsilon_h^m). \tag{41}$$

Equation (41) transforms to the usual additive decomposition of strain only for the case when all strain components are small in comparison with 1,

$$\varepsilon_h\simeq\varepsilon_h^e+\varepsilon_h^\theta+\varepsilon_h^t+\varepsilon_h^m. \tag{42}$$

Similar definitions and decompositions are valid for the deformation gradient in a binder (with $\varepsilon_b^t=0$) and for the composite. At the initial (before straining) and the current time instant we have the following expressions for the volume of composite:

$$V_0=V_{0h}+V_{0b}+V_{0v},\quad V=V_h+V_b+V_g, \tag{43}$$

where V_{0v} is the initial volume of voids in the PBX and V_g is the volume of gas which remains in the cylinder. Dividing the second Eq. (43) by V_0, we obtain for the deformation gradient of a composite

$$\begin{aligned}F&=\frac{V_h}{V_{0h}}\frac{V_{0h}}{V_0}+\frac{V_b}{V_{0b}}\frac{V_{0b}}{V_0}+\frac{V_g}{V_{0v}}\frac{V_{0v}}{V_0}\\&=F_hf_{0hv}+F_bf_{0bv}+F_gf_{0v}\\&=(F_hf_{0h}+F_bf_{0b})(1-f_{0v})+F_gf_{0v},\end{aligned} \tag{44}$$

where $F_g=V_g/V_{0v}$ is the deformation gradient of the gas with respect to the initial volume of voids V_{0v}, and the initial volume fractions of the HMX and binder with respect to void-free PBX, f_{0h} and f_{0b}, are related to the initial volume fractions with respect to porous PBX f_{0hv} and f_{0hv} by Eq. (29): $f_{0hv}=f_{0h}(1-f_{0v})$ and $f_{0bv}=f_{0b}(1-f_{0v})$. The term $1-f_{0v}$ in Eq. (44) can be considered as the deformation gradient (and $-f_{0v}$ as the corresponding strain) which transforms initially porous PBX to void free PBX. Equations (40) (and a similar equation for the binder) and (44) are the main and exact kinematic relationships for our model. Note that all volume fractions in Eq. (44) correspond to initial states and are constants. Strains due to the chemical decomposition of the HMX and binder as well as due to gas accumulation in the cylinder are fully taken into account in F_h^m, F_b^m, and F_g.

In order to complete the model of PBX thermomechanical behavior, we will now describe all strain components of the HMX and binder. The elastic strain is determined by the Hooke's law

$$\varepsilon_h^e=-p/K_h,\quad \varepsilon_b^e=-p/K_b, \tag{45}$$

where $K_h=15$ GPa (Refs. 14 and 15) and $K_b=3.65$ GPa.[30] The thermal expansion strain for HMX is

$$\varepsilon_h^\theta=c\varepsilon_\delta^\theta+(1-c)\varepsilon_\beta^\theta=\varepsilon_\beta^\theta+c(\varepsilon_\delta^\theta-\varepsilon_\beta^\theta), \tag{46}$$

$$\varepsilon_\beta^\theta = 13.1 \times 10^{-5}(\theta - 300), \quad \varepsilon_\delta^\theta - \varepsilon_\beta^\theta = 0.4 \times 10^{-5}(\theta - 432), \tag{47}$$

where thermal expansion coefficients are taken from Ref. 19 and the change in thermal expansion strain at phase equilibrium temperature is zero because it is taken into account in the transformation strain $\varepsilon^t = 0.08$. The thermal expansion coefficients for the binder are unknown and we will take $\varepsilon_b^\theta = 6 \times 10^{-5}(\theta - 300)$. This indeterminacy is not critical because the thermal strain is negligible in comparison with the strain due to the binder decomposition.

VII. MODELS FOR CHEMICAL DECOMPOSITION OF THE HMX AND BINDER AND GAS LEAKING

One of the most advanced kinetic models for HMX decomposition was presented in Refs. 31 and 32. It was coupled to mechanical equations and used in Ref. 33 to model thermal explosion. The kinetic model includes four steps: (1) $\beta \rightarrow \delta$ PT, (2) decomposition of δ phase in solid state (initial ring- and bond-breaking steps), (3) decomposition of solid intermediates into gaseous intermediates (CH_2O, N_2O, HCN, HNO_2, etc.), and (4) decomposition of gaseous intermediates into final product (CO_2, H_2O, N_2, CO, etc.). Decomposition of various binders was modeled by single-step first-order Arrhenius kinetics. The goal of the earlier papers was to describe experiments on time to thermal explosion. Several decomposition models have been analyzed and compared in Ref. 5. Again, calibration of material parameters was based on comparison with experimental data on time to thermal explosion and temperature. Our goal is completely different: to describe the kinetics of $\beta \leftrightarrow \delta$ PTs under complex pressure-temperature paths. In these paths, temperature variation is prescribed and pressure is determined from the solution of the mechanical problem in which chemical decomposition, gas leaking, and mechanical strains are taken into account. For our problem, we do not need to take into account heat of all reactions because temperature evolution is prescribed. We need to consider only processes which affect the pressure variation. Thus, the step (2) can be neglected because it changes the mechanical properties of the δ phase only, but these changes are unknown. The step (4) can be neglected as well, since it changes the equation of state of the gaseous mixture, which is also quite hypothetical.[33] Since step (1) is described in this paper by physically based kinetics which is much more precise, we need to describe step (3) of HMX decomposition and find kinetic parameters in first-order Arrhenius equation for nitroplasticizer and Estane decomposition with emphases on mass loss rather than heat of reaction. That is why we will use here our kinetic data from Refs. 34 and 35 that were obtain in the following way. First, parameters in kinetic Eqs. (48) and (49) for decomposition of nitroplasticizer and Estane are determined to fit thermogravimetric data (i.e., mass loss) in Refs. 34 and 35 (Fig. 5). Note that in Ref. 34, two-step kinetic equations are used but we do not need the kinetics of decomposition of the gaseous intermediates of nitroplasticizer into final product gases [similar to step (4) for HMX] because the difference in equation of state for them is not well known.

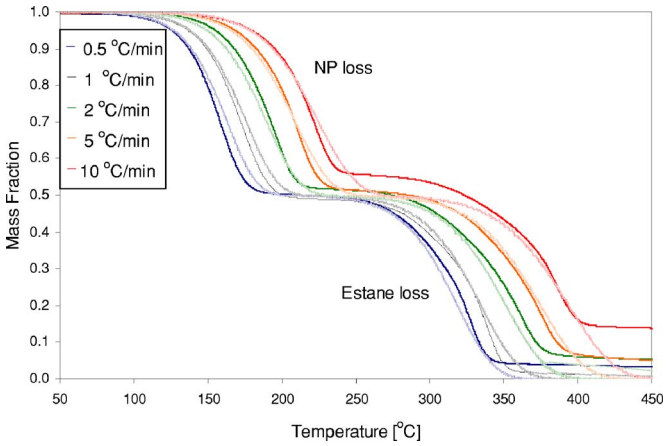

FIG. 5. (Color online) Thermogravimetric analysis (TGA) data to measure solid mass loss from binder components nitroplasticizer and Estane in a 50:50 mixture by mass (solid lines) (Ref. 35). The TGA data were obtained in an open platinum pan using an INSTRUMENTX for five different temperature ramp rates. Dashed lines represent results of simulation based on Eqs. (48) and (49).

Then parameters of the second-order kinetic Eq. (52) are determined from the condition that in combination with Eqs. (48) and (49) for binder decomposition, it fits thermogravimetric data for PBX 9501 in Refs. 34 and 35 (Fig. 6).

A. Chemical decomposition of the nitroplasticizer and Estane and corresponding strains

Kinetic equations for nitroplasticizer and Estane decomposition are given below[34,35]

$$\dot{\phi}_{N/b} = -k_N \phi_{N/b}, \quad k_N = \exp(14.30)\exp\left(-\frac{80000}{R\theta}\right), \tag{48}$$

$$\dot{\phi}_{E/b} = -k_N \phi_{E/b}, \quad k_E = \exp(16.52)\exp\left(-\frac{120500}{R\theta}\right). \tag{49}$$

Here $\phi_{N/b}$ and $\phi_{E/b}$ are the mass fractions of the nitroplasticizer and Estane with respect to the initial total mass of the binder; their initial values are $\phi_{N/b}(0) = \phi_{E/b}(0) = 0.5$; time is measured in seconds. The strains in the nitroplasticizer, Es-

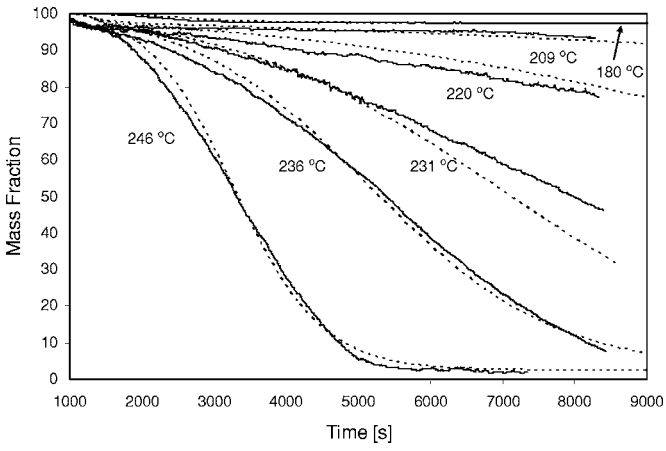

FIG. 6. Isothermal thermogravimetric analysis data (solid lines) to measure solid mass loss from PBX 9501, i.e., combined mass loss from the binder and HMX. Dashed lines represent results of simulation based on Eqs. (48), (49), and (52).

tane, and binder due to mass loss during the chemical decomposition are

$$\varepsilon_N^m = (0.5 - \phi_{N/b})\rho_b/\rho_N, \quad \varepsilon_E^m = (0.5 - \phi_{E/b})\rho_b/\rho_E,$$

$$\varepsilon_b^m = \varepsilon_N^m + \varepsilon_E^m. \tag{50}$$

Indeed, $\varepsilon_N^m := \Delta V_N/V_b = (\rho_N \Delta V_N/\rho_b V_b)(\rho_b/\rho_N) = (\Delta m_N/m_b) \times (\rho_b/\rho_N) = (0.5 - \phi_{N/b})(\rho_b/\rho_N)$, where ΔV_N and Δm_N are the volume and mass loss of the nitroplasticizer due to chemical decomposition. A similar equation is valid for the Estane. Also, $\varepsilon_b^m = (\Delta V_N + \Delta V_b)/V_b = \varepsilon_N^m + \varepsilon_E^m$.

Kinetic Eqs. (48) and (49) adequately reproduce the experimental data in Ref. 35 (Fig. 5). Since decomposition of the Estane is important above 520 K only, which is above the temperature range of interest, we will neglect it and use $\varepsilon_b^m = \varepsilon_N^m$. At constant heating rate, h_r and $\theta = \theta_{\text{in}} + h_r t$, Eq. (48) can be integrated in the closed form

$$\phi_{N/b} = \phi_{N/b}(\theta_{\text{in}}) \exp\left\{\frac{A}{h_r}\left[\exp\left(-\frac{B}{\theta_{\text{in}}}\right)\theta - \exp\left(-\frac{B}{\theta}\right)\theta + BEi\left(-\frac{B}{\theta_{\text{in}}}\right) - BEi\left(-\frac{B}{\theta}\right)\right]\right\}, \tag{51}$$

where $A = \exp(14.3) = 1.623 \times 10^6$, $B = 80\,000/R = 9622.5$ K, h_r is measured in K/s and $Ei(z) = -\int_{-z}^{\infty} e^{-t}/t\,dt$ $(z < 0)$ is the exponential integral function. Note that in calculations we use $\phi_{N/b}(\theta_{\text{in}}) = 0.500001$ to avoid the numerical problems related to zero strains at θ_{in}. A similar equation is valid for $\phi_{E/b}$.

B. Chemical decomposition of the HMX and corresponding strain

The kinetics of HMX decomposition into gas product can be described by the following equation:[34,35]

$$\dot{f}_{hv} = -k_h f_{hv}(1 - f_{hv}\rho_h/\rho_{Pv}),$$

$$k_h = 3.769 \times 10^9 \theta \exp\left(\frac{-150\,000}{R\theta}\right),$$

$$f_{hv}(0) = f_{0hv} = 0.95(1 - f_{0v})\rho_P/\rho_h, \quad \varepsilon_h^m = f_{hv}/f_{0hv} - 1 \le 0, \tag{52}$$

where f_{hv} is the current volume fraction of the HMX (remaining unloaded volume of the HMX divided by the initial unloaded volume of the PBX), $\rho_h = 1905$ kg/m^3 and $\rho_{Pv} = \rho_P(1 - f_{0v})$ are the initial mass densities of HMX and PBX; the initial volume fraction of HMX, f_{0hv}, is determined using Eqs. (28) and (29): $f_{0hv} = \phi_{0h}(1 - f_{0v})\rho_P/\rho_h$. For $f_{0v} = 0.015 - 0.02$ we obtain $\rho_{Pv} = 1832 - 1823$ kg/m^3 and $\rho_h/\rho_{Pv} = 1.039 - 1.045$. The solution of Eq. (52) is in good agreement with our experimental data. Also, the solution of a combination of Eqs. (50) and (52) describes our experimental data on the combined mass loss of the HMX and the binder well (Fig. 6).

C. Equation of state of a gas phase

We will assume in the first approximation that gas which appears due to decomposition of the nitroplasticizer and HMX can be described by the ideal gas equation of state and that the volume of both gases is additive (Amagat–Leduc law[36])

$$V_g = V_{gh} + V_{gb} = \left(\frac{m_{gh}}{M_{gh}} + \frac{m_{gb}}{M_{gb}}\right)\frac{R\theta}{p}, \tag{53}$$

where V_{gh} and V_{gb} are the partial volumes of gas product due to decomposition of the HMX and nitroplasticizer, m_{gh} and m_{gb} are the corresponding masses, and M_{gh} and M_{gb} are the corresponding molecular masses. We will assume $M_{gh} = M_{gb} = 0.037$ kg/mol. For HMX, it is based on the average of the molecular masses of CH_2O and N_2O which are typical decomposition intermediates. Expressing masses of gases in terms of mass fractions, ϕ_{gh} and ϕ_{gb}, with respect to initial mass of PBX, m, i.e., $m_{gh} = \phi_{gh} m$ and $m_{gb} = \phi_{gb} m$, we obtain for the deformation gradient of the gas

$$F_g = \frac{V_g}{V_{0v}} = \left(\frac{\phi_{gh}}{M_{gh}} + \frac{\phi_{gb}}{M_{gb}}\right)\frac{R\theta m}{pV_{0v}}, \tag{54}$$

Since $m = \rho_{Pv} V_0 = \rho_P(1 - f_{0v})V_0 = \rho_P(1 - f_{0v})V_{0v}/f_{0v}$, then

$$F_g f_{0v} = \frac{Q}{p}(1 - f_{0v}), \quad Q = \left(\frac{\phi_{gh}}{M_{gh}} + \frac{\phi_{gb}}{M_{gb}}\right)R\theta\rho_P. \tag{55}$$

D. Gas leaking rule

We will use the following equation for the gas leaking from the cylinder:

$$\dot{\phi}_g^- = 0 \quad \text{for} \quad p \le p_s,$$

$$\dot{\phi}_g^- = 2.25lJ(p - p_s) \quad \text{for} \quad p_s < p \le 1.8p_s,$$

$$\dot{\phi}_g^- = lJp \quad \text{for} \quad p \ge 1.8p_s,$$

$$J = \phi_g/f^* \quad \text{for} \quad 0 \le \phi_g \le f^*, \quad J = 1 \quad \text{for} \quad \phi_g > f^*. \tag{56}$$

Here ϕ_g^- is the mass fraction of the gas (relative to the initial mass of the PBX) which leaked from the cylinder, $\phi_g = \phi_{gh} + \phi_{gb}$ is the current mass fraction of the gas in the cylinder, p_s is the threshold pressure of the gas above which leaking is possible, l is the choked leak rate coefficient, and J is a function described later. The leaking is absent if pressure is below the threshold value p_s that depends on the sealing system. At higher pressure, the leak rate is proportional to the overpressure $p - p_s$. If the pressure is higher than $1.8p_s$, then the leak rate is independent of the threshold p_s and is proportional to p. Factor 2.25 for the coefficient l is obtained from the continuity of the $\dot{\phi}_g^-$ for $p = 1.8p_s$. This equation is motivated by a one-dimensional isentropic analysis of ideal gas flow: the mass flow rate is independent of the pressure outside the system as long as $p/p_s > 1.8$.

Without the function J, Eq. (56) exhibits leaking even if there is no gas in a cylinder (i.e., $\phi_g = 0$) since pressure can

be higher than p_s; recall that we assume the same pressure in the gas and solid. The simplest way to avoid this is to put $J=0$ for $\phi_g=0$ and $J=1$ for $\phi_g>0$. However, in this case J (and consequently the rate of leaking) experiences multiple jumps between 0 and 1 during numerical solution of Eq. (56) which depends on the parameters and the numerical methods. To avoid this, we use a better expression for J: J varies linearly from 0 to 1 in a small interval of $0\le\phi_g\le f^*$ (e.g., $f^*=10^{-3}-10^{-4}$) and then remains equal to 1. Such a function not only regularizes the numerical procedure but also mimics real physics that for a small amount of gas in the cylinder, pressure in gas can be much smaller than in the solid and disappears when gas disappears.

E. Mass fraction of gas in a cylinder

The total mass fraction of gas in the cylinder, ϕ_g, is the difference between the gas input due to HMX and nitroplasticizer decomposition [see Eqs. (48) and (52)] and the gas loss due to leaking, i.e.,

$$\phi_g = 0.5(L_g + |L_g|) = \phi_{gb} + \phi_{gh}, \tag{57}$$

$$L_g := (0.5 - \phi_{N/b})0.05 + \left[0.95 - \frac{f_{hv}\rho_h}{\rho_P(1-f_{0v})}\right] - \phi_g^-. \tag{58}$$

It is easy to show that $f_{hv}\rho_h/\rho_P(1-f_{0v})$ is the current mass fraction of HMX: according to Eqs. (28) and (29), $\phi_h=\rho_h f_h/\rho_P=f_{hv}\rho_h/\rho_P(1-f_{0v})$. Equation (57) guarantees the nonnegativity of ϕ_g when L_g is getting formally negative due to intensive gas leak. To decompose ϕ_g into ϕ_{gh} and ϕ_{gb}, we assume that gas product of the nitroplasticizer and HMX leak in the same proportion as they are produced, i.e.,

$$\phi_{gb} = \phi_g \frac{(0.5 - \phi_{N/b})0.05}{(0.5 - \phi_{N/b})0.05 + \{0.95 - (f_{hv}\rho_h)/[\rho_P(1-f_{0v})]\}}, \tag{59}$$

$$\phi_{gh} = \phi_g \frac{0.95 - (f_{hv}\rho_h)/[\rho_P(1-f_{0v})]}{(0.5 - \phi_{N/b})0.05 + \{0.95 - (f_{hv}\rho_h)/[\rho_P(1-f_{0v})]\}}. \tag{60}$$

For the case $M_{gh}=M_{gb}$, one gets $Q=(\phi_g/M_{gh})R\theta\rho_P$ and there is no need to separate ϕ_g into ϕ_{gh} and ϕ_{gb} and using Eqs. (59) and (60).

F. Pressure evolution in a cylinder

We will consider the following problem. Let the cylindrical PBX sample be placed into a rigid cylinder and an initial macroscopic compressive strain $\varepsilon_0=F_0-1<0$ be prescribed by the piston motion (Fig. 4). Then the sample is homogeneously heated at the heating rate h_r during which ε_0 is kept constant. During the heating, the following processes occur: thermal expansion, binder melting, chemical decomposition of the binder and HMX, $\beta\to\delta$ PT, gas leak, and elastic straining.

Pressure can be determined from Eq. (44) after substitution of the multiplicative decomposition of F_h [Eqs. (40) and (41)] and similar equation for F_b, Eq. (55) for $F_g f_{0v}$, as well as $F=F_0$ and Hooke's law Eq. (45),

$$F_0 = [(1 - p/K_h)F_{hi} + (1 - p/K_b)F_{bi} + Q/p](1 - f_{0v}),$$

$$F_{hi} = F_h^\theta F_h^t F_h^m f_{0h}, \quad F_{bi} = F_b^\theta F_b^m f_{0b}, \tag{61}$$

where F_{hi} and F_{bi} are inelastic deformation gradients in the HMX and the binder. Solving Eq. (61) for p one obtains

$$p = \frac{HK_bK_h + \sqrt{H^2K_b^2K_h^2 + 4QS}}{2S}, \quad S = F_{hi}K_b + F_{bi}K_h,$$

$$H = F_{hi} + F_{bi} - F_0/(1 - f_{0v}). \tag{62}$$

It is clear that prestraining F_0 and the porosity $1-f_{0v}$ contribute to the pressure through the combination $F_0/(1-f_{0v})\simeq 1+\varepsilon_0+f_{0v}$. Since ε_0 and f_{0v} have different signs, they partially or completely compensate each other. If one considers ε_0 as variable strain, then Eq. (62) represents a volumetric strain-pressure equation of state for the composite material under consideration.

VIII. CONCLUDING REMARKS

The main results of this paper are:

(a) Elaborating a suggested nucleation mechanism for the $\beta\to\delta$ PT in the energetic crystal HMX in the presence of a liquid binder.
(b) Development of the fully physical model for the overall kinetics of the $\beta\leftrightarrow\delta$ PTs for complex pressure-temperature paths based on the earlier nucleation mechanism and the growth mechanism via the virtual melting.
(c) Development of simple phenomenological models for the HMX, nitroplasticizer, and Estane chemical decomposition and gas leaking.
(d) Development of the coupled thermomechanochemical model for a composite consisting of crystalline HMX embedded in a binder (PBX formulation) under thermomechanical loading. It takes into account all the earlier mentioned processes and an exact large strain kinematics.

Numerical analysis of the heating of PBX 9501 inside of a rigid cylinder based on the developed model will be presented in the accompanying paper.[12] The effect of the heating rate, initial porosity, and prestraining, HMX and binder decomposition and gas leaking rule on the kinetics of the $\beta\leftrightarrow\delta$ PT and pressure buildup will be analyzed numerically.

ACKNOWLEDGMENTS

V.I.L acknowledges the LANL Contract Nos. (13720-001-05-AH and 31553-002-06) and NSF Grant Nos. (CMS-02011108 and CMS-0555909); B.F.H., L.B.S., and B.W.A. acknowledge the support of the Laboratory Research and Development and H.E. Science Programs at Los Alamos National Laboratory. The main part of this work has been performed during V.I.L.'s sabbatical leave at LANL. The hospitality of L.B.S., B.F.H., B.W.A., and D.K.Z. is very much appreciated.

[1]B. W. Asay, G. Parker, P. Dickson, B. Henson, and L. Smilowitz, J. Energ. Mater. **22**, 223 (2004).
[2]B. F. Henson, L. B. Smilowitz, B. W. Asay, and P. M. Dickson, J. Chem. Phys. **117**, 3780 (2002).
[3]L. B. Smilowitz, B. F. Henson, B. W. Asay, and P. M. Dickson, J. Chem. Phys. **117**, 3789 (2002).
[4]A. K. Burnham, R. K. Weese, and B. L. Weeks, J. Phys. Chem. B **108**, 19432 (2004).
[5]A. P. Wemhoff, A. K. Burnham, and A. L. Nichols, J. Phys. Chem. A **111**, 1575 (2007).
[6]R. J. Karpowicz and T. B. Brill, AIAA J. **20**, 1586 (1982).
[7]J. C. Gump and S. M. Peiris, J. Appl. Phys. **97**, 053513 (2005).
[8]V. I. Levitas, B. F. Henson, L. B. Smilowitz, and B. W. Asay, Phys. Rev. Lett. **92**, 235702 (2004).
[9]V. I. Levitas, L. B. Smilowitz, B. F. Henson, and B. W. Asay, Appl. Phys. Lett. **87**, 191907 (2005).
[10]V. I. Levitas, B. F. Henson, L. B. Smilowitz, and B. W. Asay, J. Phys. Chem. B **110**, 10105 (2006).
[11]V. I. Levitas, L. B. Smilowitz, B. F. Henson, and B. W. Asay, J. Chem. Phys. **124**, 026101 (2006).
[12]V. I. Levitas, B. F. Henson, L. B. Smilowitz, D. K. Zerkle, and B. W. Asay, J. Appl. Phys. (submitted).
[13]V. I. Levitas, L. B. Smilowitz, B. F. Henson, and B. W. Asay, Appl. Phys. Lett. **89**, 231930 (2006).
[14]R. Menikoff and T. D. Sewell, Combust. Theory Modell. **6**, 103 (2002).
[15]T. D. Sewell, R. Menikoff, D. Bedrov, and G. D. Smith, J. Chem. Phys. **119**, 7417 (2003).
[16]H. H. Cady and L. C. Smith, Studies on the Polymorphs of the HMX, LAMS-2652, 1962.
[17]A. S. Teetsov and W. C. McCrone, Microscope **15**, 13 (1965).
[18]R. K. Weese and A. K. Burnham, Propellants, Explos., Pyrotech. **30**, 344 (2005).
[19]M. Herrmann, W. Engel, and N. Eisenreich, Propellants, Explos., Pyrotech. **17**, 190 (1992).
[20]H. H. Cady, 17th International Annual Conference of ICT, Karlsruhe, FRG, 1986, pp. 17.1–17.12.
[21]J. L. Lyman, Y. C. Liau, and H. V. Brand, Combust. Flame **130**, 185 (2002).
[22]L. B. Smilowitz, B. F. Henson, M. Greenfield, A. Sas, B. W. Asay, and P. M. Dickson, J. Chem. Phys. **121**, 5550 (2004).
[23]D. A. Porter and K. E. Easterling, *Phase Transformations in Metals and Alloys* (Van Nostrand Reinhold, London, 1989).
[24]G. G. Hammes, *Principles of Chemical Kinetics* (Academic, New York, 1978).
[25]B. F. Henson, B. W. Asay, R. K. Sander, S. F. Son, J. M. Robinson, and P. M. Dickson, Phys. Rev. Lett. **82**, 1213 (1999).
[26]R. M. Christensen, *Mechanics of Composite Materials* (Wiley, New York, 1979).
[27]R. Hill, *Mathematical Theory of Plasticity* (Clarendon, Oxford, 1950).
[28]V. I. Levitas, Int. J. Solids Struct. **35**, 889 (1998).
[29]V. I. Levitas, *Large Deformation of Materials with Complex Rheological Properties at Normal and High Pressure* (Nova Science, New York, 1996).
[30]B. Clements, private communication.
[31]C. M. Tarver, J. Energ. Mater. **22**, 93 (2004).
[32]C. M. Tarver and T. D. Tran, Combust. Flame **137**, 50 (2004).
[33]J. J. Yoh, M. A. McClelland, J. L. Maienschein, A. L. Nichol, and C. M. Tarver, J. Appl. Phys. **100**, 073515 (2006).
[34]D. K. Zerkle and B. W. Asay, Nuclear Weapons J. **1**, 12 (2006).
[35]L. Davis, private communication.
[36]J. P. Holman, *Thermodynamics* (McGraw-Hill, New York, 1974).